Journal of Magnetic Resonance 207 (2010) 206–212

Contents lists available at ScienceDirect

Journal of Magnetic Resonance

journal homepage: www.elsevier.com/locate/jmr

2_4-SEMA as a sensitive and offset compensated SLF sequence

S. Jayanthi [a], N. Sinha [b,*], K.V. Ramanathan [c,**]

[a] Department of Physics, Indian Institute of Science, Bangalore 560 012, India
[b] Centre of Biomedical Magnetic Resonance, Sanjay Gandhi Post Graduate Institute of Medical Sciences Campus, Raebareli Road, Lucknow 226 014, India
[c] NMR Research Centre, Indian Institute of Science, Bangalore 560 012, India

ARTICLE INFO

Article history:
Received 28 May 2010
Revised 23 August 2010
Available online 28 September 2010

Keywords:
2_4-SEMA
PISEMA
SAMPI4
Transverse spin-lock
Sensitivity enhancement and offset compensation

ABSTRACT

Separated Local Field (SLF) spectroscopy is a powerful tool for the determination of structure and dynamics of oriented systems such as membrane proteins oriented in lipid bilayers and liquid crystals. Of many SLF techniques available, Polarization Inversion Spin Exchange at Magic Angle (PISEMA) has found wide application due to its many favorable characteristics. However the pulse sequence suffers from its sensitivity to proton resonance frequency offset. Recently we have proposed a new sequence named 2_4-SEMA (J. Chem. Phys. 132 (2010) 134301) that overcomes this problem of PISEMA. The present work demonstrates the advantage of 2_4-SEMA as a highly sensitive SLF technique even for very large proton offset. 2_4-SEMA has been designed for obtaining reliable dipolar couplings by switching the magic-angle spin-lock for protons over four quadrants as against the use of only two quadrants in PISEMA. It is observed that for on-resonance condition, 2_4-SEMA gives rise to signal intensity comparable to or slightly higher than that from PISEMA. But under off-resonance conditions, intensities from 2_4-SEMA are several fold higher than those from PISEMA. Comparison with another offset compensated pulse sequence, SAMPI4, also indicates a better intensity profile for 2_4-SEMA. Experiments carried out on a single crystal of ^{15}N labeled N-acetyl–DL-valine and simulations have been used to study the relative performance of the pulse sequences considered.

1. Introduction

Dipolar couplings provide structural information due to their dependence on molecular orientation and inter-atomic distances. They are also sensitive to molecular dynamics and can provide information about local motion. There exist a wide range of NMR methods which help in extracting heteronuclear dipolar coupling in the solid state which are known as Separated Local Field (SLF) techniques [1,2]. SLF experiment resolves in two dimensions heteronuclear dipolar couplings on the basis of the chemical shifts. Such experiments are used extensively to characterize the structure of magnetically and mechanically oriented membrane proteins in lipid bilayers [3–11] and also to study liquid crystalline systems [12–14]. Out of the several possible SLF methods available for measuring dipolar couplings, the technique Polarization Inversion Spin Exchange at Magic Angle (PISEMA) [15,16] is being used extensively. This technique utilizes the exchange of spin polarization between ^{1}H and a low γ nucleus such as ^{15}N. In this experiment, during t_1, proton magnetization is spin-locked along an effective field at the magic angle. ^{15}N magnetization also remains spin-locked at the Hartman–Hahn match during this time period with phases following the proton. During spin exchange, magnetization evolves under the heteronuclear dipolar couplings while the homonuclear dipolar couplings are removed. For efficient removal of proton homonuclear dipolar couplings there exist many effective methods [17–22]. Out of these Lee–Goldburg (LG) homonuclear decoupling sequence [17] provides efficient averaging of the couplings and a large scaling factor. Though robust in several aspects, the major disadvantage of PISEMA is that the measured dipolar couplings depend largely on the proton offsets. This may be a major limitation of this sequence for experiments performed at higher magnetic fields. Especially in the case of proteins, where amide proton chemical shifts span a range of about 14 ppm, the effects are very significant [23,24]. To address this issue, several approaches have been proposed in the literature [25–28]. One such pulse sequence that retains the advantage of PISEMA (Fig. 1a) and at the same time removes its proton offset dependence is the recently reported SLF sequence, 2_4-SEMA [29] (Fig. 1). The sequence is designed in such a way that the effective field is cycled through all the four quadrants during t_1 evolution (Fig. 1b), whereas in PISEMA it is cycled only through two quadrants (Fig. 1a). Switching the effective field through all the quadrants has been achieved by changing the offset and r.f. phase of the spin-lock appropriately.

* Corresponding author. Fax: +91 522 266 8215.
** Corresponding author. Fax: +91 802 360 1550.
E-mail addresses: neeraj.sinha@cbmr.res.in (N. Sinha), kvr@sif.iisc.ernet.in (K.V. Ramanathan).

1090-7807/$ - see front matter © 2010 Elsevier Inc. All rights reserved.
doi:10.1016/j.jmr.2010.08.019

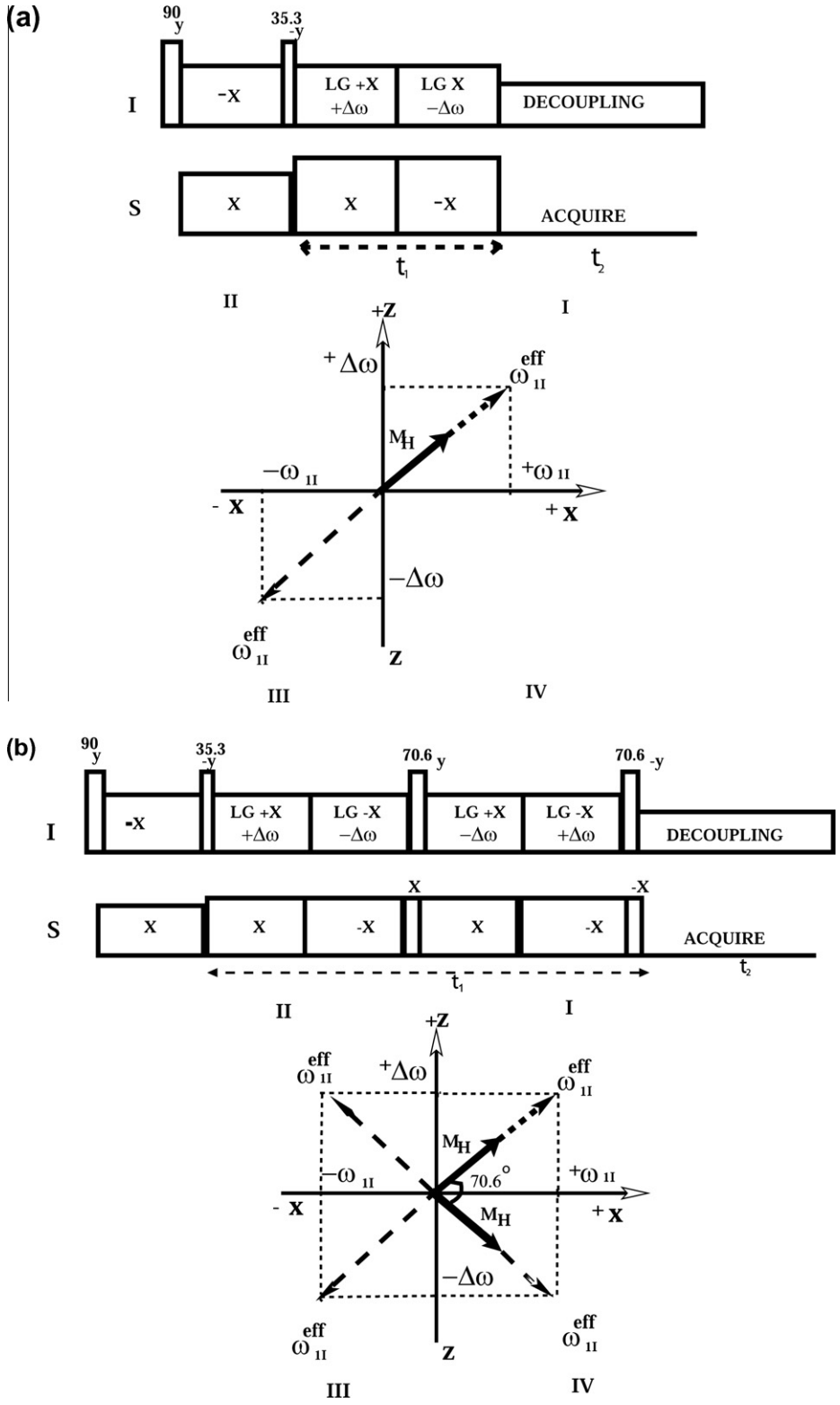

Fig. 1. (a) PISEMA and (b) 2_4-SEMA pulse sequence with their respective effective fields.

Proton magnetization is appropriately switched to retain the spin-lock with the use of additional 70.6° pulses. Since the magnetization is switched between two quadrants and the effective field between all the four quadrants in one t_1 evolution, the sequence is named as 2_4-SEMA, where '2' represents the magnetization and the subscript, '4' represents the effective field. Contrary to the expectation that the efficiency of homonuclear decoupling might deteriorate with the insertion of additional on-resonance pulses in the middle of the decoupling sequence for back and forth switching of magnetization, we have observed with 2_4-SEMA good resolution and sensitivity for the peaks even at extreme proton offsets. This is a feature which was not reported earlier.

The difficulties that limit solid state NMR in structure determination are (i) the requirement of large amount of samples for better S/N, (ii) heat induced by the r.f. especially on heat sensitive samples like membrane proteins oriented in lipid bilayers and (iii) dependence of the pulse sequence to external parameters like Hartmann–Hahn match, proton chemical shifts etc. Towards sensitivity enhancement, it is noteworthy to mention the recent work on inclusion of paramagnetic centers in membrane proteins oriented in lipid bilayers [30]. The present work deals with the effectiveness of 2_4-SEMA pulse sequence in retaining the sensitivity of the dipolar doublets even at extreme proton offsets. We compare the performance of this sequence with PISEMA and another offset compensated SLF sequence, SAMPI4 [26,27]. The experiments have been carried out on a single crystal of a model peptide, ^{15}N labeled N-acetyl-DL- valine (NAV). The studies are important in the context of obtaining ^{1}H–^{15}N dipolar couplings and the ^{15}N chemical shifts leading to information on the orientations of peptide planes of proteins in the applied magnetic field.

2. The pulse sequence

PISEMA utilizes frequency switched Lee–Goldburg decoupling sequence (FSLG) [18] for achieving homonuclear decoupling. The PISEMA pulse sequence is given in Fig. 1a which also shows the directions taken by the magnetization and effective field. After an initial polarization transfer, the ^{1}H (I) magnetization is spin-locked in the effective field direction for the LG decoupling sequence in the first quadrant by the application of a 35.3° pulse with phase $-Y$. After a 2π rotation of the magnetization in the first quadrant, the phase of the effective field is reversed by 180°. This is followed by another 2π rotation of the magnetization in the third quadrant. During the entire t_1 time period, ^{15}N (S) magnetization remains spin-locked at Hartmann–Hahn match with the r.f. phases following that of the proton allowing a coherent exchange of magnetization between proton and nitrogen mediated by the dipolar coupling. During t_2 period, ^{15}N magnetization is measured with proton decoupling. A two dimensional Fourier transform yields ^{15}N chemical shift along the F_2 axis and ^{1}H–^{15}N dipolar couplings along the F_1 axis. PISEMA provides relatively narrow lines along the dipolar dimension and a large scaling factor (~0.82). But the measured dipolar couplings show a dependence on the proton–offset frequency and the signal intensity deteriorates. These are seen in the expression [31] for the detected signal

$$S(t) = k\left[\frac{(\omega_{1I}^{eff} - \omega_{1S})^2 + d^2\sin^2\theta_m\cos(\omega_e^{\Delta}t)}{(\omega_e^{\Delta})^2}\right] \quad (1)$$

where $\omega_{1I}^{eff} = \sqrt{\Delta\omega^2 + \omega_{1I}^2}$ is the spin-lock field for the I spin pointing along the magic angle, ω_{1S} is the spin-lock r.f. on the ^{15}N and d is the heteronuclear dipolar coupling between ^{1}H and ^{15}N scaled by $\sin\theta_m$. The couplings are scaled due to spin-lock of the ^{1}H magnetization along the magic angle θ_m. $\omega_e^{\Delta} = \sqrt{(\omega_{1I}^{eff} - \omega_{1S})^2 + d^2\sin^2\theta_m}$ and k represents any instrument related factors. From Eq. (1) it can be shown that the measured dipolar coupling has a quadratic dependence with respect to the off-resonance value. A parabolic variation of the experimental value as a function of proton offset is observed, with the minimum of the parabola being closest to the actual dipolar coupling. To alleviate this problem of proton offset dependence, we have recently proposed a new sequence named 2_4-SEMA. The idea of super cycling the FSLG sequence has been applied by switching the LG effective field in all the four quadrants (Fig. 1b). The sequence was earlier implemented on liquid crystalline systems, between ^{1}H and ^{13}C and its robustness towards proton off-resonance was demonstrated. In this article we systematically monitor the sensitivity of the sequence as a function of proton offset for a low γ nuclei like ^{15}N in a rigid system. We also compare the main features like sensitivity and offset dependency of the sequence with PISEMA and SAMPI4.The pulse sequence 2_4-SEMA is a modification of PISEMA and is given in Fig. 1(b) along with effective field directions. For the first FSLG block, the proton offset and the r.f. phase are given by $(+\Delta\omega, +X)$ and $(-\Delta\omega, -X)$, where $\Delta\omega$ represents the LG offset which is given by $\frac{\omega_{1I}}{\sqrt{2}}$. During this period, the proton magnetization is in the magic angle direction in the first quadrant. Subsequently with a pulse of 70.6° it is switched to the fourth quadrant. It is then spin-locked with the effective field direction of FSLG block in the fourth and second quadrants, $(-\Delta\omega, +X)$ and $(\Delta\omega, -X)$. Finally the magnetization is taken back to the first quadrant by a 70.6° pulse with phase of $-Y$. This completes one super cycle which may be repeated several times during the t_1 period. The S spin phase follows the phase of the proton magnetization throughout the t_1 time period. This results in a final effective Hamiltonian which is devoid of proton offsets and r.f. inhomogeneities. At the end of the entire t_1 the final zeroth order average Hamiltonian obtained is of the form [29]

$$^{1,1,4,4}_{1,3,4,2}H^{\Delta} = (d\sin\theta_m)I_X^{\Delta} \quad (2)$$

where the superscripts and the subscripts represent respectively the quadrants the magnetization and the effective field are taken through. H^{Δ} represents the zero quantum part of the Hamiltonian for spin exchange between the isolated I–S spin pairs, I_X^{Δ} is a spin operator in this sub-space, θ_m the magic angle and d, the dipolar coupling between the I–S spin pairs. This modification under assumption of ideal flip pulses not only retains the theoretically achievable scaling factor of PISEMA but also makes the sequence devoid of any offset dependence. We have employed numerical methods, SIMPSON [32] to study the effect of the pulse sequence. The results obtained with experiment and simulation is discussed in detail in the following sections.

3. Experimental

All Experiments were performed on a Bruker Avance-III 600 MHz spectrometer equipped with 3.2 mm MAS probe under static conditions. The proton resonance frequency was 600.154 MHz and the ^{15}N resonance frequency was 60.81 MHz. Single crystal of ^{15}N-acetyl-DL-valine is taken in a 3.2 mm rotor and a static cross polarization experiment is set up between ^{1}H and ^{15}N to detect the ^{15}N nuclei. The crystal is adjusted a couple of times to get the desired orientation where four resonances in the ^{15}N can be obtained. For all 2D experiments maximum acquisition time in the t_1 domain remains identical (~4.5 ms). The r.f field used for LG decoupling for PISEMA and 2_4-SEMA was 59 kHz with a time period of 13.8 μs for each LG block. The number of points during t_1 evolution was kept 80 for PISEMA and 2_4-SEMA experiments. For SAMPI4 the t_1 points were 140 with an incremental delay of 32.08 μs. Total acquisition time in t_1 domain and total experimental time for each 2D experiment were kept identical. Hartmann–Hahn conditions and the recycle delay of 5 s were kept identical for all the sequences. 90° pulses were calibrated accurately at the saturation point of the amplifier and estimated within an error of 0.02 μs. SPINAL-128 [33] decoupling was used in the ^{1}H channel during ^{15}N detection. The 2D data matrix is double Fourier transformed with $2k$ and 256 points in the F_2 and F_1 dimensions respectively. In all cases the data in the F_1 dimension were acquired in the quadrature-off mode and processed identically. A shifted squared sine bell function was used in the F_2 dimension while no window function was employed in the F_1 dimension. For 2_4-SEMA, the 70.6° pulse was calibrated carefully for the largest power possible with the probe and was found to be 1.49 μs. F_1 axis was scaled as per the theoretical scaling factor for both

PISEMA and 2_4-SEMA experiments while no scaling was used for SAMPI4.

4. Results and discussions

The performance of the 2_4-SEMA sequence in terms of sensitivity and offset dependence were tested on a single crystal of ^{15}N labeled N-acetyl-DL-valine. The 2D spectrum of the sample with ^1H–^{15}N dipolar couplings in the F_1 dimension and ^{15}N chemical shift in the F_2 dimension is shown in Fig. 2. The ^{15}N 1D chemical shift spectrum is shown at the top of the 2D spectrum. The linewidth observed in the ^{15}N chemical shift dimension is of the order of 1.5 ppm. The four resonances arise from the four magnetically inequivalent molecules in the unit cell of NAV. It can be seen from the 2D spectrum that the peak at ~120 ppm is of low intensity possibly because of its low dipolar coupling value and hence will not be discussed further. Spectra have been obtained at three proton offsets, viz. −4, +4 and +12 ppm, of which +4 ppm corresponds to on-resonance condition. The F_1 cross-sections corresponding to the ^{15}N chemical shift at around 220 ppm (marked with a *) are shown in Fig. 3 and the ones corresponding to the peaks at 195 and 150 ppm are given in the Supplementary Information (SI – S1). The various proton offsets used for recording the respective 2D's are shown in the left most extreme of Fig. 3. From the figures it is observed that intensities obtained from the 2_4-SEMA experiment remain uniformly high for all offsets. Under on-resonance condition, PISEMA and SAMPI4 provide intensities which are at best equal to intensities obtained from 2_4-SEMA. For a proton offset of +4 ppm, for the ^{15}N peak shown in Fig. 3 (middle row), the 2_4-SEMA intensity is slightly higher by about 15% than the intensity of the PISEMA spectrum. For this proton offset, SAMPI4 spectra show slightly lower intensities compared to the other two for all the three peaks. But what is significant is that under off-resonance conditions considered here, signal from 2_4-SEMA experiment remains almost the same as that observed for on-resonance condition, whereas for other pulse sequences, the intensity reduces significantly. Thus the 2_4-SEMA spectra shown in the top and bottom rows of Fig. 3 have nearly the same intensity as that of the middle row. This is true for the other two peaks also as shown in the Supplementary Section. On the other hand, the PISEMA spectra intensities have deteriorated very significantly due to proton offset. In this case, for the peak at 150 ppm, for an offset of −4 ppm, the intensity is almost zero (vide Supplementary Section). SAMPI4 sequence also shows considerable degrading of intensity, though it is not as much as for the PISEMA. Clearly under off-resonance condition, 2_4-SEMA provides intensities which are several fold higher compared to PISEMA. A significant gain in intensity (about two times for the offset of ±8 kHz) compared to SAMPI4 is also observed. This clearly establishes the sensitivity advantage of 2_4-SEMA over the other two pulse sequence.

We have also measured the line-widths of all the peaks along the F_1 dimension for various offsets of the proton. At on-resonance (+4 ppm) the line-widths of the dipolar doublets for ^{15}N peak resonating at 220 ppm is 250, 280, 320 Hz for 2_4-SEMA, PISEMA and SAMPI4 respectively. These line-widths are slightly larger than the values reported earlier for the same sample [34], but should suffice for the purpose of comparison of the performance of the pulse sequences considered. The different line-widths for the peak

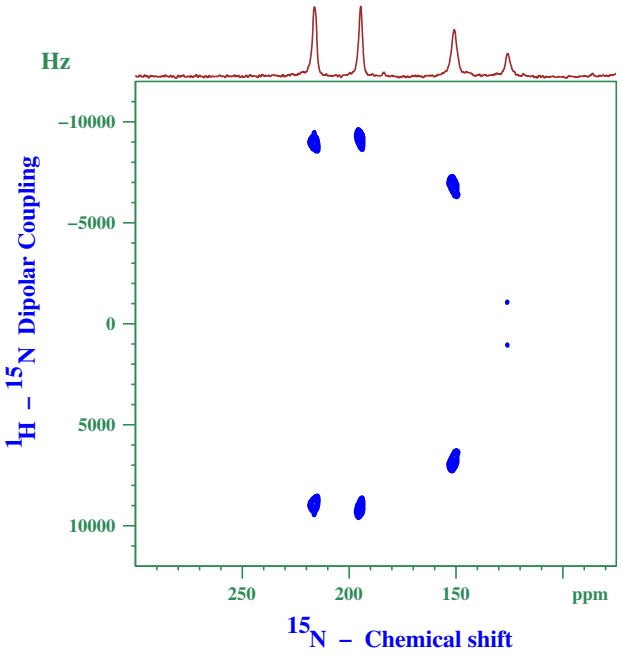

Fig. 2. 2D SLF spectra of NAV obtained with the 2_4-SEMA pulse sequence with ^1H–^{15}N dipolar couplings shown along the F_1 axis and ^{15}N chemical shift along the F_2 axis. The spectra were recorded with 80 t_1 points and a maximum of ~4.5 ms evolution time in the t_1 dimension. A total number of 12 scans per t_1 point were used with a recycle time of 5 s.

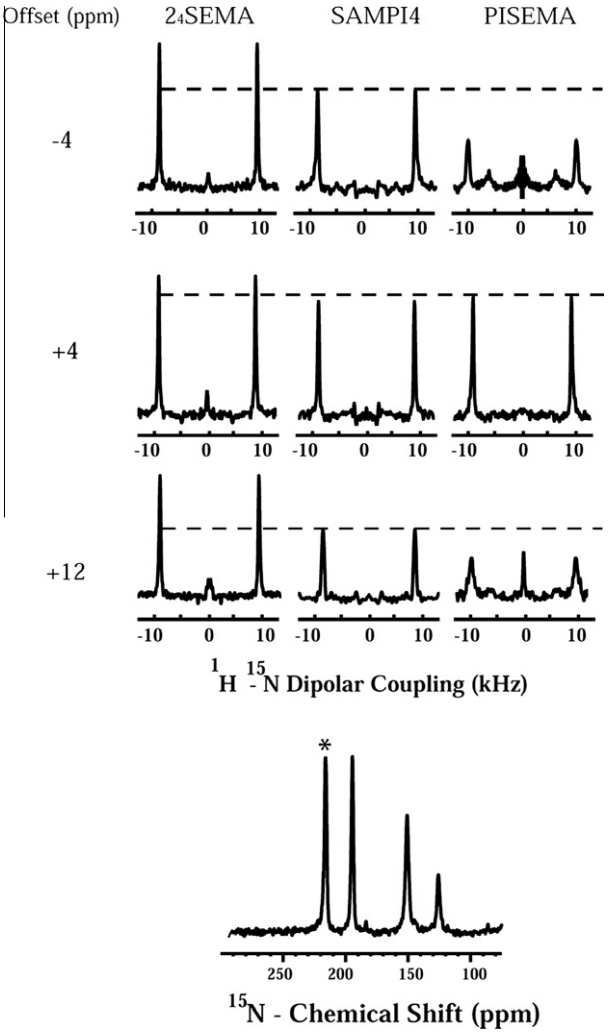

Fig. 3. Cross-section of the 2D spectra of NAV obtained using 2_4-SEMA, SAMPI4 and PISEMA at various proton offsets. The dotted line is drawn to provide a visual comparison of intensities between the three experiments. The proton offsets are (a) −4, (b) +4 and (c) +12 ppm respectively. The cross-section correspond the ^{15}N peaks with chemical shift 220 ppm (denoted by *).

at 220 ppm at different offsets for the three experiments are tabulated in Table 1. It can be seen from Table 1 that even at extreme offsets the change in the line-width of the dipolar doublets is the least for 2_4-SEMA and the highest for PISEMA. The failure of PISEMA for large offsets is possibly related to ineffectual LG decoupling, because the magic angle condition is not satisfied for large proton offsets. The loss of cross-peak intensity and the build-up of the axial peak due to proton off-resonance in PISEMA can also be seen from Eq. (1). We attribute the robustness of the new sequence to an effective transverse spin-lock of the magnetization because of the switching of the effective field in all the four quadrants. SAMPI4 also uses a transverse spin-lock and hence provides better linewidths.

We have also monitored systematically the variation of the measured dipolar coupling with respect to proton offset for the three ^{15}N peaks under 2_4-SEMA, SAMPI4 and PISEMA and the results for the ^{15}N peak resonating at 220 ppm is shown in Fig. 4. Similar results for peaks at 195 and 150 ppm are shown in the Supplementary Material. The 2D experiments have been recorded at identical conditions by varying the proton offset from −4 to +12 ppm in steps of +2 ppm. It can be seen that the measured dipolar coupling varies parabolically for PISEMA whereas for SAMPI4 it is almost linear. Most interestingly, for 2_4-SEMA the measured dipolar coupling remains constant over a large range of proton offsets. From Fig. 4 and the results shown in the Supplementary Data, it is clear that 2_4-SEMA has better offset independence compared to SAMPI4 and PISEMA.

Though 2_4-SEMA is advantageous in terms of sensitivity and offset independence as demonstrated above, one of the major issues to be considered for its optimal performance is the optimization of the flip angle of the 70.6° pulse. Since it switches the magnetization back and forth between first and the fourth quadrants, the pulse has to be calibrated with extreme precision so that the performance of the sequence is not hindered. A short pulse in the delta pulse regime is ideal, so that the magnetization evolution within the pulse can be largely avoided. This also ensures the theoretical scaling factor of 0.82 as in PISEMA. We have employed a short pulse of 1.49 μs in all the plots shown in Fig. 3. Fig. 5(i–iii) shows the experimental results for 2_4-SEMA for different pulse lengths for the 70.6° pulse. Three different pulse lengths viz., 1.49, 2.89 and 4.55 μs were used by employing different power levels, keeping the angle of the pulse the same. 2D spectra were recorded by keeping the proton off-resonance of +4 ppm and corresponding to different pulse lengths. Fig. 5(i) represents the cross-section of the dipolar doublets for ^{15}N resonating at 220 ppm for a flip angle pulse power of 132 kHz. This was the maximum power allowed as per our spectrometer and probe specifications. Second and the third columns represent the respective cross-sections for pulse powers (ii) 69 and (iii) 43 kHz respectively. It can be seen from Fig. 5 and also from the Supplementary Material that, with the reduction in pulse power, the intensities of the peaks decrease and also a zero peak appears at the centre. As the pulse power reduces, line shape also degrades significantly.

The above mentioned characteristics of 2_4-SEMA have been verified by performing a series of simulations using SIMPSON. An isolated two spin system, ^{1}H–^{15}N, with a dipolar coupling of 10 kHz is considered for numerical analysis. PISEMA and 2_4-SEMA simulations have been carried out with identical parameters. An ideal 70.6° pulse is used in the later case which only flips the magnetization from the first quadrant to the fourth quadrant. This avoids evolution of the magnetization during the pulse. Experimentally this can be mimicked to some extent by using a high power pulse. Fig. 6a and b is an overlaid plot of PISEMA and 2_4-SEMA respectively at various proton offsets. In both figures, the offset values range from on-resonance (0 ppm) to 12 ppm. Under offset variation it is seen that PISEMA plot (Fig. 6a) shows a reduction in intensity of the dipolar doublets together with an increase of the separation between the peaks and the appearance of intense zero frequency peak. In the case of 2_4-SEMA (Fig. 6b), the intensity of the dipolar doublets, the dipolar scaling factor as well as the intensity of the zero frequency peak remain essentially same for all values of the proton offset. From the above observations one may conclude that 2_4-SEMA provides better intensity profile when compared with PISEMA even at extreme proton offsets, supporting the experimental results shown in Figs. 3 and 4. Simulations have also been carried out to check the effect of the intermediate 70.6° pulse on the performance of 2_4-SEMA. The variation of the intensity of the dipolar doublets with respect to different r.f. powers for the flip angle 70.6° is given in Fig. 7. It can be seen in the figure that with the reduction of the 70.6° pulse power from 200 kHz to 50 kHz, the intensity and the scaling factor of the dipolar doublets decrease significantly. It can also be seen that the zero peak of 2_4-SEMA increases along with the increase in the pulse lengths supporting the experimental results (Fig. 5). This result may be of significance for biological samples, as achieving large r.f. fields of the order of 100 kHz for the switching pulse in the case of wet samples might be one of the challenges for the proposed technique and further studies are under progress in this direction.

It may be mentioned that there are similarities between the pulse sequence BB-PISEMA proposed earlier [25] and 2_4-SEMA proposed here. Both use r.f. pulses in between dipolar evolutions to annul effects of chemical shift dispersion. The main difference is that in the former case the effective field stays in two quadrants as in PISEMA, whereas in the latter case it is taken through all four quadrants. Therefore 2_4-SEMA could be expected to provide a better averaging over r.f. field and offset related inhomogeneities, though this has to be experimentally verified. Accurate calibration of the 180^0 pulse in the case of BB-PISEMA is also a concern in the case of large chemical shifts.

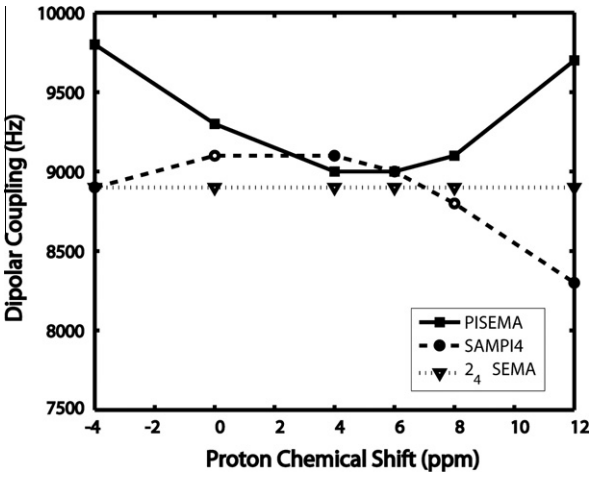

Fig. 4. Variation of the measured dipolar coupling with proton offsets evolution for the ^{15}N peak resonating at 220 ppm under the PISEMA, SAMPI4 and 2_4-SEMA.

Table 1
Full width at half height of the dipolar doublets of the peak at 220 ppm at various offsets for experiments, PISEMA, 2_4-SEMA and SAMPI4 respectively.

Proton offset	−4 ppm	+4 ppm	+12 ppm
	Full width at half height (Hz)		
2_4-SEMA	284	280	304
SAMPI4	440	320	350
PISEMA	705	250	870

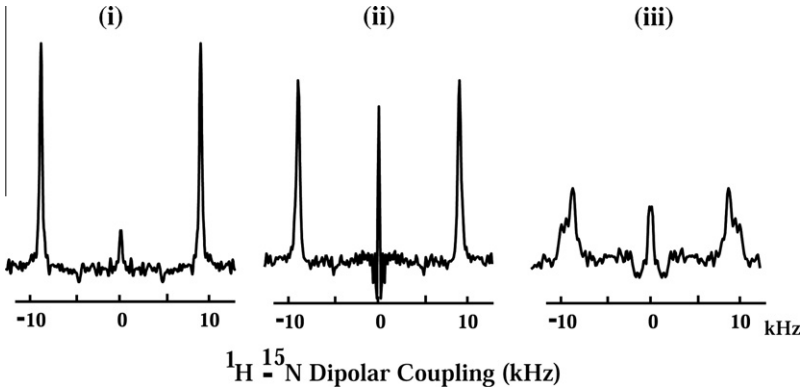

Fig. 5. F_1 cross-sections of the ^{15}N resonance at 220 ppm shown for three different values for the 70.6° pulse length in 2_4-SEMA pulse sequence: (i) 1.49, (ii) 2.82 and (iii) 4.55 μs respectively.

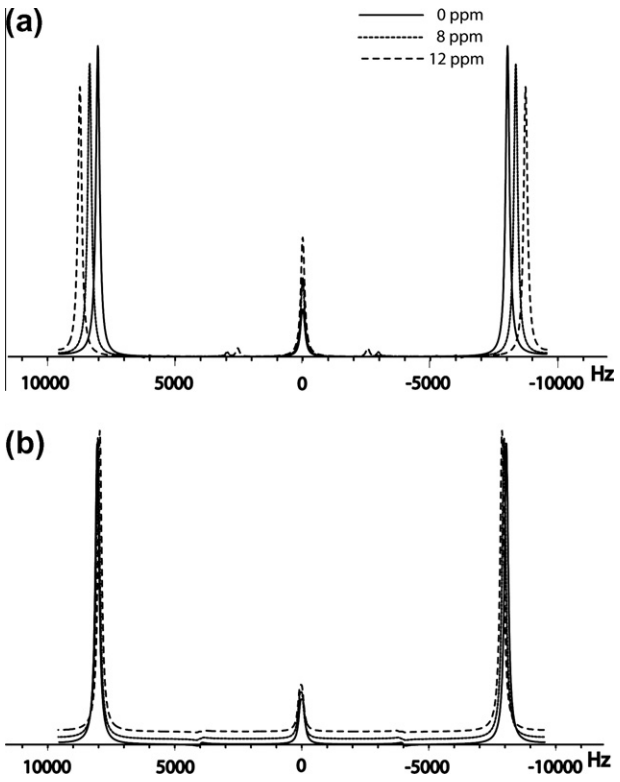

Fig. 6. Simulation plots to show the sensitivity enhancement of 2_4-SEMA for a two spin system using SIMPSON. (a) PISEMA spectrum. (b) 2_4-SEMA spectrum at proton offsets 0, +8 and +12 ppm.

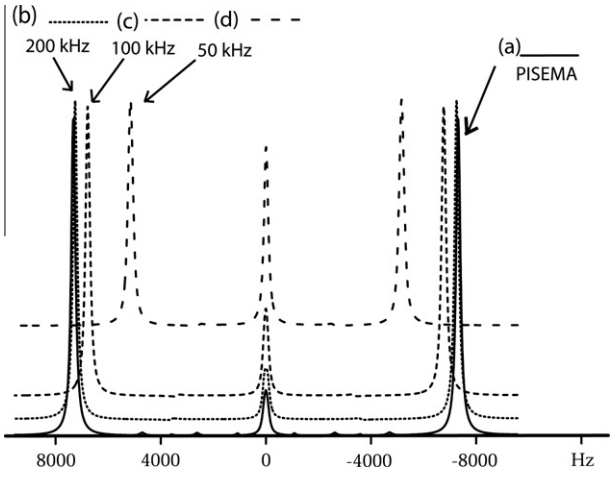

Fig. 7. SIMPSON simulation plots showing the variation of the scaling factor for the 2_4-SEMA sequence with respect to the length of the 70.6° pulse. Here (a) is the PISEMA simulation and (b)–(d) correspond to 2_4-SEMA for various r.f. power employed for the 70.6° pulse. (b) 200 kHz, (c) 100 kHz and (d) 50 kHz.

5. Conclusions

We have demonstrated the utility of a 2_4-SEMA in terms of sensitivity and offset compensation in single crystal of model peptide. We have also shown that this sequence is robust in handling extreme proton offsets without loss of sensitivity or line-widths when compared with some of the existing SLF sequences. With use of adequate r.f. power for the switching pulse, the modification does not affect the large scaling factor characteristics of PISEMA. Sensitivity loss is a serious concern at higher fields where the proton chemical dispersion increases and we believe that the proposed sequence will be of great advantage especially in membrane proteins where trans-membrane and in-plane domains are present. The concept of the recently proposed pulse sequence which increases the sensitivity of PISEMA experiments [35] may also be incorporated into 2_4-SEMA to make it uniformly sensitivity enhanced irrespective of the proton offsets. From the experimental and supporting simulations, it may be concluded that the new sequence is highly tolerant to proton offsets and preserves the sensitivity even at extreme offsets. It may however be borne in mind that it is necessary to use a short time period for the 70.6° pulse, which may not be a serious issue with today's new generation of spectrometer hardware. Though this involves an additional optimization step for the pulse sequence, the advantages of the proposed sequence such as increased sensitivity and possibility of getting dependable dipolar coupling values in a single measurement, adequately compensate for the initial loss of time.

Acknowledgments

The Solid State NMR facility, at the Centre for Biomedical Magnetic Resonance – Lucknow, India where all the experiments were carried out is gratefully acknowledged. Prof. C.L. Khetrpal, Director, CBMR is gratefully acknowledged for his support and encouragement.

Appendix A. Supplementary material

Supplementary data associated with this article can be found, in the online version, at doi:10.1016/j.jmr.2010.08.019.

References

[1] J.S. Waugh, Uncoupling of local field spectra in nuclear magnetic resonance: determination of atomic positions in solids, Proc. Natl. Acad. Sci. U. S. A 73 (1976) 1394–1397.

[2] R.K. Hester, J.L. Ackermann, B.L. Neff, J.S. Waugh, Separated local field spectra in NMR: determination of structure of solids, Phys. Rev. Lett. 36 (1976) 1081–1083.

[3] S.J. Opella, F.M. Marassi, Structure determination of membrane proteins by NMR spectroscopy, Chem. Rev. 104 (2004) 3587–3606.

[4] S.J. Opella, NMR and membrane proteins, Nat. Struct. Biol. 4 (Suppl.) (1997) 845–848.

[5] F.M. Marassi, A. Ramamoorthy, S.J. Opella, Complete resolution of the solid-state NMR spectrum of a uniformly 15N-labeled membrane protein in phospholipid bilayers, Proc. Natl. Acad. Sci. U. S. A. 94 (1997) 8551–8556.

[6] S. Dvinskikh, U. Durr, K. Yamamoto, A. Ramamoorthy, A high-resolution solid-state NMR approach for the structural studies of bicelles, J. Am. Chem. Soc. 128 (2006) 6326–6327.

[7] R. Fu, T.A. Cross, Solid-state nuclear magnetic resonance investigation of protein and polypeptide structure, Annu. Rev. Biophys. Biomol. Struct. 28 (1999) 235–268.

[8] R. Bertram, J.R. Quine, M.S. Chapman, T.A. Cross, Atomic refinement using orientational restraints from solid-state NMR, J. Magn. Reson. 147 (2000) 9–16.

[9] A. Ramamoorthy, NMR structural studies on membrane proteins, Biochim. Biophys. Acta 1768 (2007) 2947–2948.

[10] S.J. Opella, A. Nevzorov, M.F. Mesleb, F.M. Marassi, Structure determination of membrane proteins by NMR spectroscopy, Biochem. Cell Biol. 80 (2002) 597–604.

[11] T.A. Cross, C.M. Gall, S.J. Opella, NMR studies of filamentous bacteriophage assembly, Prog. Clin. Biol. Res. 64 (1981) 457–465.

[12] A. Ramamoorthy, D.K. Lee, T. Narasimhaswamy, R.P. Nanga, Cholesterol reduces pardaxin's dynamics – a barrel-stave mechanism of membrane disruption investigated by solid-state NMR, Biochim. Biophys. Acta 1798 (2010) 223–227.

[13] T. Narasimhaswamy, D.K. Lee, K. Yamamoto, N. Somanathan, A. Ramamoorthy, A 2D solid-state NMR experiment to resolve overlapping aromatic resonances of thiophene-based nematogens, J. Am. Chem. Soc. 127 (2005) 6958–6959.

[14] T. Narasimhaswamy, M. Monette, D.K. Lee, A. Ramamoorthy, Solid-state NMR characterization and determination of the orientational order of a nematogen, J. Phys. Chem. B 109 (2005) 19696–19703.

[15] C.H. Wu, A. Ramamoorthy, S.J. Opella, High-resolution heteronuclear dipolar solid-state NMR spectroscopy, J. Magn. Reson. A 109 (1994) 270–272.

[16] A. Ramamoorthy, Y.F. Wei, D.K. Lee, PISEMA solid state NMR spectroscopy, Annu. Rep. NMR Spectrosc. 52 (2004) 1–52.

[17] M. Lee, W.I. Goldburg, Nuclear magnetic resonance line narrowing by a rotating r.f. field, Phys. Rev. 140 (1965) A1261–1271.

[18] A. Bielecki, C.A. Kolbert, M.H. Levitt, Frequency switched pulse sequences: homonuclear decoupling and dilute spin NMR in solids, Phys. Lett. 155 (1989) 341–346.

[19] J.S. Waugh, L.M. Huber, U. Haeberlen, Approach to high resolution NMR in solids, Phys. Rev. Lett. 20 (5) (1968) 180–182.

[20] D.P. Burum, M. Linder, R.R. Ernst, Low-power multipulse line narrowing in solid-state NMR, J. Magn. Reson. 44 (1) (1981) 173–188.

[21] K. Takegoshi, C.A. McDowell, A "magic echo" pulse sequence for the high-resolution NMR spectra of abundant spins in solids, Chem. Phys. Lett. 116 (2–3) (1985) 100–104.

[22] M. Howhy, P.V. Bower, H.J. Jakobsen, N.C. Nielsen, A highorder and broadband CRAMPS experiment using *z*-rotational decoupling, Chem. Phys. Lett. 273 (5–6) (1997) 297–303.

[23] R. Gerald, T. Bernhard, U. Haeberlen, J. Rendell, S.J. Opella, Chemical shift and electric field gradient tensors for the amide and carboxyl hydrogens in the model peptide N-acetyl-D-L-valine. Single-crystal deuterium NMR study, J. Am. Chem. Soc. 115 (1993) 777–782.

[24] C.H. Wu, A. Ramamoorthy, L.M. Gierasch, S.J. Opella, Simultaneous characterization of the amide ^{1}H chemical shift, ^{1}H–^{15}N dipolar and ^{15}N chemical shift interaction tensors in a peptide bond by three dimensional solid state NMR spectroscopy, J. Am. Chem. Soc. 117 (1995) 6148–6149.

[25] K. Yamamoto, D.K. Lee, A. Ramamoorthy, Broadband PISEMA solid state NMR spectroscopy, Chem. Phys. Lett. 407 (2005) 289–293.

[26] A.A. Nevzorov, S.J. Opella, A magic sandwich pulse sequence with reduced offset dependence for high-resolution separated local field spectroscopy, J. Magn. Reson. 164 (2003) 182–186.

[27] A.A. Nevzorov, S.J. Opella, Selective averaging for high-resolution solid-state NMR spectroscopy of aligned samples, J. Magn. Reson. 185 (2007) 59–70.

[28] S.V. Dvinskikh, K. Yamamoto, A. Ramamoorthy, Heteronuclear isotropic mixing separated local field NMR spectroscopy, J. Chem. Phys. 125 (2006) 034507–034519.

[29] S. Jayanthi, K.V. Ramanathan, 2(*n*)-SEMA – a robust solid state nuclear magnetic resonance experiment for measuring heteronuclear dipolar couplings in static oriented systems using effective transverse spin-lock, J. Chem. Phys. 132 (2010) 134501–134509.

[30] K. Yamamoto, J. Xu, K.E. Kawulka, J.C. Vederas, A. Ramamoorthy, Use of copper-chelated lipid speeds up NMR measurements from membrane proteins, J. Am. Chem. Soc. 132 (2010) 6929–6931.

[31] Z. Gan, Spin dynamics of polarization inversion spin exchange at the magic angle in multiple spin systems, J. Magn. Reson. 143 (2000) 136–143.

[32] M. Bak, J.T. Rasmussen, N.C. Nielsen, SIMPSON: a general simulation program for solid-state NMR spectroscopy, J. Magn. Reson. 147 (2000) 296–330.

[33] B.M. Fung, A.K. Khitrin, K. Ermolaev, J. Magn. Reson. 142 (2000) 131–140.

[34] C.H. Wu, S.J. Opella, Proton detected separated local field spectroscopy, J. Magn. Reson. 192 (2008) 165–170.

[35] T. Gopinath, G. Veglia, Sensitivity enhancement in static solid-state NMR experiments via single- and multiple-quantum dipolar coherences, J. Am. Chem. Soc. 131 (2009) 5754–5756.